

Weighing in Motion of Railway Vehicles: Development of Innovative Systems and Performance Analysis

A. Innocenti*, L.Marini*, E.Meli*, L.Pugi*, A.Rindi*

* Department of Industrial Engineering
University of Florence
via di S.Marta 3, 50139, Italy
enrico.meli@unifi.it

ABSTRACT

The accurate estimation of the axle loads and the correct detection of overloads and imbalances, represent a primary concern for railways management companies, since they are strictly related to traffic safety and maintenance planning of the track. *Weigh in Motion* (WIM) systems aim at the dynamic weighing of railway vehicles through a reasonable number of measurement stations placed along the track. Such systems may overcome disadvantages in terms of costs and traffic management exhibited by conventional static weighing systems.

In this paper the authors present an innovative algorithm for high speed WIM applications to estimate the wheel loads of trains by means of indirect track measurements. The formulation of the algorithm is quite general and it can be customized for several track measurements; consequently it can be employed in different typologies of measurement stations. The WIM algorithm processes the set of experimental physical quantities chosen as track inputs by means of estimation procedures based on least square (LSQ) minimization techniques. The vertical loads on the train wheels are computed from the measurements according to the assumption that the effects of the single wheel loads on the track are approximately superimposable. The whole WIM architecture has been developed in cooperation with Ansaldo STS and ECM SpA.

1 INTRODUCTION

The dynamical weighing of moving vehicles can be conveniently carried out through specialized measurement stations, without stopping the circulating vehicles as it must be done when performing static weighing. In that regard, an increasing interest is addressed to the development of efficient and reliable versions of such measurement systems, usually referred to as *Weigh in Motion* (WIM) systems from both the railway industry and the scientific community [7, 3, 11, 9]. The crucial aspects of each WIM system are the performance of the measurement station and the features of the algorithm employed to perform the assessment of the unknown wheel or axle loads. In the present paper the authors introduce an innovative algorithm [7, 3, 11, 9] for the wheels or axle loads estimation that may be accomplished by exploiting different types of track measurements such as rail shear, rail bending, vertical forces on the sleepers or even by means of any their combination. The innovative WIM algorithm estimates the vertical load of each wheel from indirect rail measurements assuming that the effects of the single wheel loads on the track are approximately superimposable (quasi-linearity hypothesis). Thanks to the previous assumption, the track response to the transit of the whole train (i.e. indirect rail measurements chosen as inputs) may be expressed as an appropriate weighted combination of the effects provided by a series of single nominal loads moving along the track at the vehicle speed. Then, the set of physical quantities selected as track inputs are properly processed by the WIM algorithm through estimation procedures based on least square (LSQ) minimisation techniques [10].

Thanks to its accuracy, the developed WIM algorithm is able to perform also the estimation of the longitudinal X_G and lateral Y_G coordinates of the center of mass of the vehicle starting from the estimated vertical loads acting on the wheels. The developed WIM algorithm can manage both real experimental data or simulated data. The simulated data are provided by a physical model of the railway track that has been developed expressly to test the WIM algorithm with a suitable simulation campaign when experimental data are not available. The new algorithm has been tested through numerical simulations performed using an architecture composed of a detailed 3D multibody model of a two-boogies railway vehicle and of an accurate finite

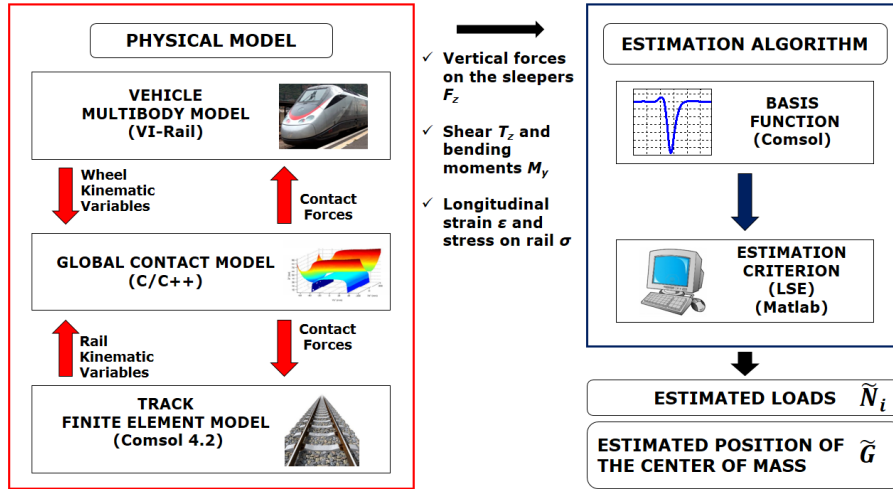


Figure 1. General architecture of the model used in the development of the WIM system.

element model of a flexible ballasted track. To reproduce real conditions, both physical noise and measurement noise have been included in the developed model. Several running conditions have been reproduced to verify the robustness of the WIM algorithm performances in several operating conditions, characterized by different values of the parameters that influence the dynamic response of the track (vehicle speed, car body mass, load distribution etc.). The whole WIM architecture has been developed in cooperation with Ansaldo STS and ECM SpA.

2 General architecture of the system

The general architecture of the developed WIM algorithm [9] is illustrated in Fig. 1 and it consists of two main parts: the physical model and the estimation algorithm. The purpose of this arrangement consists in the chance of testing the algorithm performance also when experimental data are not available: the necessary track inputs are provided by the dedicated mechanical model through numerical simulations of a completely known vehicle transiting on the track. Such simulations are performed to obtain the dynamic response of the track in terms of the specific physical inputs chosen to be used in the estimation process. More precisely, the physical model is formed of two sub-models: the multibody model of the investigated vehicle (implemented in Adams VI-Rail environment) and the finite element model of the track (developed in Comsol environment) that, during the dynamic simulation, interact online through a global contact model developed and validated by the authors in previous works [8, 1]. At each time integration step the multibody model of the vehicle evaluates the kinematic variables (position, orientation and their derivatives) relative to the wheelset and consequently to each wheel. Meanwhile the finite element track model evaluates the kinematic variables (position, orientation and their derivatives) of each rail. Rail and wheel kinematic variables are sent as inputs to the global contact model that calculates the global contact forces and sends these values back both to the vehicle multibody model and to the finite element track model. The estimation part is made up of the innovative algorithm (implemented in Matlab) and the module for the basis functions evaluation (developed in Comsol) described in chapter 4. As previously introduced, the structure of the estimation algorithm is general and it can manage different kind of physical inputs or even a combination of them. It requires some additional information concerning the vehicle speed V , the axle number n_{tot} and positions along the railway vehicle x_{ai} with $i = 1, \dots, n_{tot}$ that can be measured through the utilization of additional sensors or transmitted by the vehicle by means of low cost technologies. In this work the algorithm is based on the measurement of the vertical forces acting on the sleepers performed by means of force sensitive elements placed over the sleepers in the section corresponding to the rail baseplate/pads. These forces (simulated F_{zr}^{fn}, F_{zl}^{fn} if provided by a physical model of the railway track or real F_{zr}^{sp}, F_{zl}^{sp} if coming from experimental data), represent the physical track inputs of the WIM algorithm that, starting from the knowledge of these quantities, estimates the wheel or axle loads \hat{N} , longitudinal \hat{X}_G and lateral \hat{Y}_G

position of the center of mass G of the investigated vehicle, through suitable estimation procedures derived from the least squares minimization [12][6][10].

3 Physical model of the railway track

To generate suitable simulations to test the WIM algorithm when experimental data are not available, a model involving all the components of track structure and vehicle is required. The physical model consists of a 3D finite element model of the infrastructure (rail, sleepers and ballast), a 3D multibody model of the vehicle and an innovative 3D wheel-rail contact model. In the rest of the paper x_{ai} denotes the initial position of the i -th axle of the vehicle (the total number of the axles is n_{tot}), while the generic vertical right and wheel loads are indicated as N_{Ri} and N_{Li} . The corresponding estimated wheel loads \hat{N}_{Ri} and \hat{N}_{Li} will be computed by the presented WIM algorithm; the weights of the wheelsets are included in the loads \hat{N}_{Ri} and \hat{N}_{Li} .

Rails are modelled as 6 degrees of freedom 3D beams, connected through visco-elastic elements to n_{sl} 2D rigid bodies representing rail sleepers, which are in turn supported by a visco-elastic foundation including the ballast properties. The visco-elastic elements include lateral k_{ysl} , vertical k_{zsl} and rotational $k_{\vartheta sl}$ stiffness and lateral c_{ysl} , vertical c_{zsl} and rotational $c_{\vartheta sl}$ damping properties. The generic 2D sleeper is supported by a flexible foundation characterising the behaviour of the ballast through the lateral k_{ybal} , vertical k_{zbal} and rotational $k_{\vartheta bal}$ stiffness values and lateral c_{ybal} , vertical c_{zbal} and rotational $c_{\vartheta bal}$ damping values. The 3DOF system modelling the sleepers-ballast ensemble is described by the lateral y_{sl} and vertical z_{sl} translations and the rotation ϑ_{sl} around the x_{sl} -axis of the sleeper reference system. More details on the modelling and on the parameters of the rail-sleeper-ballast ensemble can be found in [2].

The investigated vehicle chosen for the dynamic simulations is the Manchester Wagon whose mechanical structure and elastic and damping characteristics are easily available in literature [4, 2]. The vehicle is composed of the car body, two bogies and four wheelsets. For further detail on the multibody 3D model of this vehicle one can refer to [2]. The vehicle model and the infrastructure model interact online during the simulations by means of a 3D global contact model, specifically developed to improve reliability and accuracy of the contact points detection. In particular the adopted contact model is based on a two step procedure; the contact points detection [8, 1] and the global contact forces evaluation [5].

The numerical results have been obtained using the IDA solver, which uses variable order variable step size backward differentiation formulas (BDF) for the time integration; the algorithm MUMPS has been employed to solve the linear systems arising from the FE discretisation of the rail beams [12][6]. The maximum step size $MaxStep$, the absolute and relative tolerance $AbsTol$, $RelTol$ and the maximum dimension h_{max} of the element of the rails mesh are respectively equal to 10^{-4} s, 10^{-5} (-), 10^{-6} (-) and 10^{-3} m. The processor used in the simulations is an INTEL Xeon CPU X 5690 - 3.47 GHz, 24GB RAM.

To improve the accuracy of the physical model of the railway track, two kind of disturbances have been taken into account. Firstly the frequency effects on the generic considered input signals T_r , T_l due to the limited band of physical system and measurement chain are introduced. These effects have been modelled through a second order low pass filter directly applied to the physical signals T_{rk}^{sim} , T_{lk}^{sim} relative to the measure points x_{rk} and x_{lk} (with subscripts r and l denoting respectively right and left measurement point) of the measurement station: $T_{rk}^f(t) = B_{2,\omega_n}(s)T_{rk}^{sim}(t)$ and $T_{lk}^f(t) = B_{2,\omega_n}(s)T_{lk}^{sim}(t)$ where $B_{2,\omega_n}(s)$ is the second order Butterworth filter and $\omega_n = 2\pi f_n$ is the cut frequency (ω_n in rad/s and f_n in Hz). Besides the frequency effects, also numerical disturbances and bias errors on the signal T_{rk}^f, T_{lk}^f have been modelled: $T_{rk}^{fn}(t) = T_{rk}^f(t) + U_{Tr}[\mu_{Tr}, \delta_{Tr}/2]$ and $T_{lk}^{fn}(t) = T_{lk}^f(t) + U_{Tl}[\mu_{Tl}, \delta_{Tl}/2]$ where μ_{Tr}, μ_{Tl} and $\delta_{Tr}/2, \delta_{Tl}/2$ are the means and the standard deviations of the disturbance distributions U_{Tr}, U_{Tl} . The aim of numerical disturbances and bias errors on the signals T_{rk}^{fn}, T_{lk}^{fn} is to reproduce the numerical noise affecting the measurement.

4 WIM algorithm

4.1 Vertical wheel loads estimation

The WIM algorithm (see Fig. 2) may operate both with generic simulated (\mathbf{T}_{rk}^{fn} and \mathbf{T}_{lk}^{fn}) and experimental (\mathbf{T}_{rk}^{sp} and \mathbf{T}_{lk}^{sp}) input data. The developed algorithm performs the estimation of the vertical right \hat{N}_{Ri} and left \hat{N}_{Li} wheel loads starting from the specific track measurements chosen as input signals \mathbf{T}_{rk} and \mathbf{T}_{lk} (simulated \mathbf{T}_{rk}^{fn} and \mathbf{T}_{lk}^{fn} , if provided by the physical model, or real experimental data \mathbf{T}_{rk}^{sp} and \mathbf{T}_{lk}^{sp}) measured respectively at x_{rk} and x_{lk} , representing the abscissas of the right and of the left side of the k -th measurement point (with $k = 1, \dots, N_m$; N_m is the number of measurement points). The WIM algorithm requires some additional information concerning the investigated vehicle: vehicle speed V , the axle number n_{tot} and the axle positions inside the railway vehicle x_{ai} with $i = 1, \dots, n_{tot}$ must be known. These supplementary physical quantities may be identified by means of additional sensors or may be transmitted by the vehicle itself to the WIM station through low cost technologies. The main idea on which the new WIM algorithm arises, is that it results quite intuitive to suppose the system approximatively linear with respect to the vertical loads N_{Ri} , N_{Li} with $i = 1, \dots, n_{tot}$ (the *quasi-linearity hypothesis* (QLH)); in other words the effect of the generic load N_{Ri} and N_{Li} on the generic track measurement input \mathbf{T}_{rk} and \mathbf{T}_{lk} is assumed not to be affected by the presence of other loads (especially the contiguous ones). Evidently the *quasi-linearity hypothesis* (QLH) must hold within the whole range of velocities V and cut frequencies f_n considered for the studied systems. Then, the application of the superposition principle allows the track inputs \mathbf{T}_{rk} and \mathbf{T}_{lk} (both the simulated \mathbf{T}_{rk}^{fn} and \mathbf{T}_{lk}^{fn} and the experimental ones $\mathbf{T}_{rk}^{fn sp}$ and $\mathbf{T}_{lk}^{fn sp}$) produced by the whole train to be estimated.

According to the QLH hypothesis, the track inputs \mathbf{T}_{rk} and \mathbf{T}_{lk} are respectively estimated through a linear combination of $2n_{tot}$ track fictitious input signals (namely the basis functions) produced by $2n_{tot}$ single fictitious loads N_f (one for each vehicle wheel) properly shifted in the time of a delay t_i . The fictitious load N_f must include the weight of the wheel itself. In this case the linear combination coefficients are equal to \hat{N}_{Ri}/N_f and \hat{N}_{Li}/N_f . Obviously, since the system can be assumed only approximatively linear, a *Least Squares Optimization* (LQSO) is needed to minimize the approximation error and, at the same time, to optimize the values of \hat{N}_{Ri} and \hat{N}_{Li} .

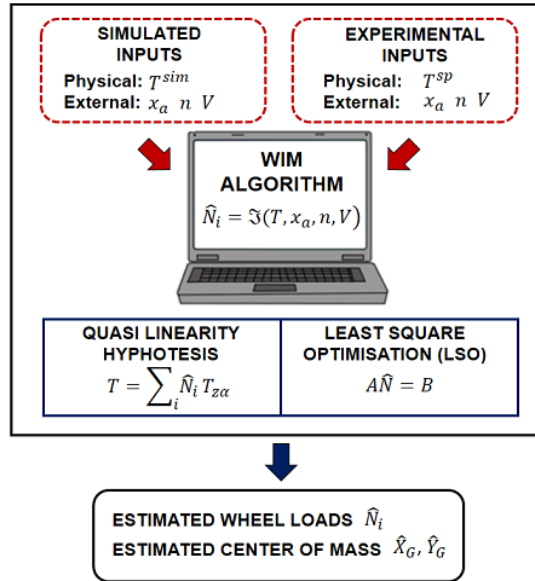


Figure 2. Architecture of the WIM algorithm

The presented WIM algorithm takes into account the coupling effect between the left and the right rail deformation caused by the dynamical behaviour of the sleeper-ballast ensemble. In the most general version of the WIM estimation procedure, track basis functions due to the transit of both left and right fictitious loads or a combination of them may be considered. More specifically, the quantities \mathbf{B}_{Ri}^{rk} and \mathbf{B}_{Li}^{rk} represent the

chosen track fictitious response due to the transit of the i -th fictitious load respectively on the right or on the left (denoted respectively with subscripts R and L) rail, measured at the right (r) side of the k -th measurement point. Analogously, \mathbf{B}_{Ri}^{rk} and \mathbf{B}_{Li}^{lk} indicate the chosen track responses due to the transit of the i -th fictitious load respectively on the right or on the left rail, measured at the left (l) side of the k -th measurement station.

The model of the rail infrastructure used in the fictitious system to evaluate the basis function is analogous to the one adopted to simulate the real physical model (see chapter 3) but, at the same time, it is quite simpler (only the vertical DOFs of rails, sleepers and ballast are considered). In fact, in real applications, the exact physical model is unknown and only a simplified approximate model can be used inside the WIM algorithm. Moreover, since the WIM procedure has to be fast and implemented almost in real-time, the fictitious model needed to evaluate the basis functions has to be necessarily simple.

For sake of clarity, the WIM algorithm estimation procedure will be described considering general track inputs \mathbf{T}_{rk} and \mathbf{T}_{lk} , but it is worthwhile noticing that the following expressions hold both for simulated (\mathbf{T}_{rk}^{fn} and \mathbf{T}_{lk}^{fn}) or experimental \mathbf{T}_{rk}^{sp} and \mathbf{T}_{lk}^{sp} track inputs. The right \mathbf{T}_{rk} and left \mathbf{T}_{lk} track inputs measured at the k -th measurement point will be expressed as $\mathbf{T}_{rk}(t) = \mathbf{T}_{rk}(x_{rk}, t)$ $\mathbf{T}_{lk}(t) = \mathbf{T}_{lk}(x_{lk}, t)$ with $t \in [T_l, T_f]$.

The position of a generic fictitious load N_f along the track is defined as $x_f = x_{af} + t * V$ (where $x_{af} = 0$ m). Consequently the $2n_{tot}$ right-side fictitious track inputs \mathbf{B}_{Ri}^{rk} and \mathbf{B}_{Li}^{rk} and the $2n_{tot}$ left-side fictitious track inputs \mathbf{B}_{Ri}^{lk} and \mathbf{B}_{Li}^{lk} (in the present case the vertical forces acting on the sleepers) produced by $2n_{tot}$ single fictitious loads can easily be assessed by introducing suitable time delays $t_i = (x_{ai} - x_{af})/V$ and by applying such delays to the track responses to the transit of a single fictitious load (i.e single wheel transit): $\mathbf{B}_{Ri}^{rk}(t) = \mathbf{B}_R^{rk}(t + t_i)$, $\mathbf{B}_{Li}^{rk}(t) = \mathbf{B}_L^{rk}(t + t_i)$, $\mathbf{B}_{Ri}^{lk}(t) = \mathbf{B}_R^{lk}(t + t_i)$ and $\mathbf{B}_{Li}^{lk}(t) = \mathbf{B}_L^{lk}(t + t_i)$ where $t \in [T_l, T_f - t_i]$. At this point, thanks to the superposition principle, the track inputs \mathbf{T}_{rk} \mathbf{T}_{lk} (both the simulated \mathbf{T}_{rk}^{fn} \mathbf{T}_{lk}^{fn} and the experimental ones \mathbf{T}_{rk}^{sp} \mathbf{T}_{lk}^{sp}) produced by the transit of the entire train can be approximated according to the following expressions:

$$\mathbf{T}_{rk}(t) \approx \mathbf{T}_{rk\ app}(t) = \sum_{i=1}^{n_{tot}} \mathbf{B}_{Ri}^{rk} \alpha_{Ri} + \sum_{i=1}^{n_{tot}} \mathbf{B}_{Li}^{rk} \alpha_{Li} \quad (1)$$

$$\mathbf{T}_{lk}(t) \approx \mathbf{T}_{lk\ app}(t) = \sum_{i=1}^{n_{tot}} \mathbf{B}_{Ri}^{lk} \alpha_{Ri} + \sum_{i=1}^{n_{tot}} \mathbf{B}_{Li}^{lk} \alpha_{Li} \quad (2)$$

where a direct proportionality between the linear combination coefficients α_{Ri} α_{Li} , the estimated vertical loads \hat{N}_{Ri} \hat{N}_{Li} and the fictitious vertical load \hat{N}_f holds: $\alpha_{Ri} = \hat{N}_{Ri}/N_f$ and $\alpha_{Li} = \hat{N}_{Li}/N_f$.

To take into account the sampling process, the time domain $t \in [T_l, \bar{T}_F]$, $\bar{T}_F = T_f - t_1$ (the shortest one among the domains $t \in [T_l, \hat{T}_F]$, $\hat{T}_F = T_f - t_i$) has been discretized with a sample time Δt . Therefore, the \mathbf{T}_{rk} \mathbf{T}_{lk} track inputs (both the simulated \mathbf{T}_{rk}^{fn} \mathbf{T}_{lk}^{fn} track inputs and the experimental ones \mathbf{T}_{rk}^{sp} \mathbf{T}_{lk}^{sp}) are known only at the times t_h with $h = 1, 2, \dots, n_s$ (n_s is the samples number while $t_1 = T_l$ and $t_{n_s} = \bar{T}_F$). The same time discretization holds also for the fictitious track outputs \mathbf{B}_{Ri}^{rk} , \mathbf{B}_{Li}^{rk} , \mathbf{B}_{Ri}^{lk} , \mathbf{B}_{Li}^{lk} employed to estimate \mathbf{T}_{rk}^{fn} , \mathbf{T}_{lk}^{fn} or \mathbf{T}_{rk}^{sp} , \mathbf{T}_{lk}^{sp} .

Re-arranging equations (1,2) in matrix form, the following expressions can be written: $\mathbf{T}_{rk} \approx \mathbf{B}_R^{rk} \alpha_R + \mathbf{B}_L^{rk} \alpha_L$ and $\mathbf{T}_{lk} \approx \mathbf{B}_R^{lk} \alpha_R + \mathbf{B}_L^{lk} \alpha_L$ where $k = 1, \dots, N_m$, $\mathbf{T}_{rk}, \mathbf{T}_{lk} \in \mathbb{R}^{n_s \times 1}$, $\mathbf{B}_R^{rk}, \mathbf{B}_L^{rk}, \mathbf{B}_R^{lk}, \mathbf{B}_L^{lk} \in \mathbb{R}^{n_s \times n_{tot}}$ and $\alpha_R, \alpha_L \in \mathbb{R}^{n_{tot} \times 1}$. Considering then the N_m measuring points, a more compact problem formulation can be obtained: $\mathbf{T}_r \approx \mathbf{B}_R^r \alpha_R + \mathbf{B}_L^r \alpha_L$ and $\mathbf{T}_l \approx \mathbf{B}_R^l \alpha_R + \mathbf{B}_L^l \alpha_L$, where $\mathbf{T}_r, \mathbf{T}_l \in \mathbb{R}^{n_s N_m \times 1}$, $\mathbf{B}_R^r, \mathbf{B}_L^r, \mathbf{B}_R^l, \mathbf{B}_L^l \in \mathbb{R}^{n_s N_m \times n_{tot}}$ and $\alpha_R, \alpha_L \in \mathbb{R}^{n_{tot} \times 1}$. The following expression finally holds:

$$\begin{bmatrix} \mathbf{T}_r \\ \mathbf{T}_l \end{bmatrix} = \begin{bmatrix} \mathbf{B}_R^r & \mathbf{B}_L^r \\ \mathbf{B}_R^l & \mathbf{B}_L^l \end{bmatrix} \begin{bmatrix} \alpha_R \\ \alpha_L \end{bmatrix} \quad (3)$$

or, more briefly, $\mathbf{T} = \mathbf{B} \alpha$ where $\mathbf{T} \in \mathbb{R}^{2n_s N_m \times 1}$, $\mathbf{B} \in \mathbb{R}^{2n_s N_m \times 2n_{tot}}$ and $\alpha \in \mathbb{R}^{2n_{tot} \times 1}$.

The estimation procedure is performed considering the coupling between the rails due to the dynamical behavior of the sleepers/ballast ensemble and taking into account the influence, on a specific measurement point, of the transit of both right and left loads. If the track model considered for the basis function evaluation exhibits some asymmetric features, the resulting estimation matrix \mathbf{B} is asymmetric, whereas if the track model is completely symmetrical, the \mathbf{B} matrix is a symmetrical block matrix with $\mathbf{B}_R^r = \mathbf{B}_L^l^T$.

Since the studied problem is only approximatively linear, a *Least Squares Optimization* (LSQO) is necessary to minimize the approximation error between \mathbf{T}_{rk} , \mathbf{T}_{lk} and $\mathbf{T}_{rk\ app}$, $\mathbf{T}_{lk\ app}$ and, at the same time, to optimize the values of \hat{N}_{Ri} , \hat{N}_{Li} . In this specific case linear not-weighted least squares have been considered [12][6][10].

In the present research activity the vertical forces acting on the sleepers (denoted with $\mathbf{F}_{z\ rk}^{fn}$ and $\mathbf{F}_{z\ lk}^{fn}$) have been adopted as track inputs. Furthermore, to simulate the sampling due to the measurement process, the time domain $t \in [T_I, \bar{T}_F]$ has been discretized with a sample time equal to $\Delta t = 0.001s$. For the simulated vertical forces acting on the sleepers $\mathbf{F}_{z\ rk}^{fn}$ and $\mathbf{F}_{z\ lk}^{fn}$, equation (3) becomes: $\mathbf{F}^{fn} = B\alpha^{sim}$. By means of a *least squares optimization* (LQSO) (in this case linear and not-weighted), it is now possible to minimize the squared 2-norms $E^{fn2} = \|\mathbf{E}^{fn}\|_2^2$ of the approximation errors $\mathbf{E}^{fn} = B\alpha^{sim} - \mathbf{F}^{fn}$. This leads to $\alpha^{sim} = (B^T B)^{-1} B^T \mathbf{F}^{fn}$ where the matrix $B^T B$ is invertible if and only if the rank of B is maximum. Finally the values of the estimated vertical loads \hat{N}_{Ri}^{sim} , \hat{N}_{Li}^{sim} can be computed starting from the knowledge of α^{sim} :

$$\alpha^{sim} = \hat{\mathbf{N}}^{sim} / N_f \quad (4)$$

where

$$\hat{\mathbf{N}}^{sim} = \begin{bmatrix} \hat{\mathbf{N}}_R^{simT} & \hat{\mathbf{N}}_L^{simT} \end{bmatrix}^T \quad (5)$$

with

$$\hat{\mathbf{N}}_R = [\hat{N}_{R1}^{sim} \quad \hat{N}_{R2}^{sim} \quad \hat{N}_{R3}^{sim} \quad \hat{N}_{R4}^{sim}]^T \quad (6)$$

$$\sum \hat{\mathbf{N}}_L = [\hat{N}_{L1}^{sim} \quad \hat{N}_{L2}^{sim} \quad \hat{N}_{L3}^{sim} \quad \hat{N}_{L4}^{sim}]^T. \quad (7)$$

4.2 Center of gravity estimation

As previously stated, the innovative WIM algorithm, starting from the estimated wheel loads \hat{N}_{Ri} and \hat{N}_{Li} , is able to evaluate the lateral Y_G and X_G longitudinal coordinates of the vehicle center of gravity (see for example Fig. 3 where a two-bogies four-axles vehicle is schematically illustrated).

Considering the horizontal plane containing the center of gravity of the railway vehicle and introducing the reference system shown in Fig.3 (the origin O coincides with the geometric center of the carbody), the moment equilibrium around X_B - axis and Y_B - axis can be respectively expressed as $\sum_{i=1}^{n_{tot}} (b_R \hat{N}_{Ri} + b_L \hat{N}_{Li}) = 0$ and $\sum_{i=1}^{n_{tot}} a_i (\hat{N}_{Ri} + \hat{N}_{Li}) = 0$.

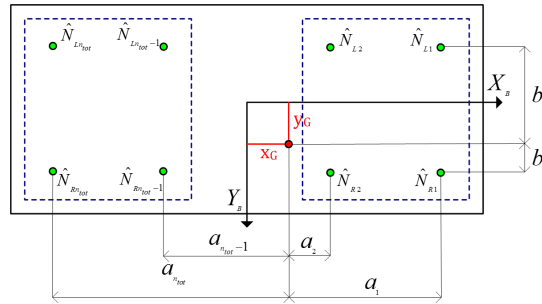


Figure 3. Evaluation of lateral and longitudinal coordinates of the vehicle center of gravity.

Taking into account the nominal values of the geometrical quantities of the vehicle such as the longitudinal position inside the train of each axle x_{ai} and the distance between the nominal rolling radius (axle track) s , the coefficients b_R , b_L and a_i can be re-written as function of the COG coordinates X_G , Y_G . More specifically, the coefficients b_R , b_L has the following expression: $b_R = \frac{s}{2} - Y_G$ and $b_L = -\frac{s}{2} - Y_G$ whereas the coefficients a_i can be calculated as follows: $a_1 = -(x_{a1} - x_{a4})/2 + X_G = c_1 + X_G$, $a_2 = -(x_{a2} - x_{a3})/2 + X_G = c_2 + X_G$,

$a_3 = (x_{a2} - x_{a3})/2 + X_G = c_3 + X_G$ and $a_4 = (x_{a1} - x_{a4})/2 + X_G = c_4 + X_G$. At this point, the moment equilibrium equations can be re-written as: $C\hat{\mathbf{G}} = \mathbf{d}$ where $C \in \mathbb{R}^{2 \times 2}$, $\hat{\mathbf{G}}, \mathbf{d} \in \mathbb{R}^2$ and

$$C = \begin{bmatrix} \sum_{i=1}^{n_{tot}} (\hat{N}_{Ri} + \hat{N}_{Li}) & 0 \\ 0 & -\sum_{i=1}^{n_{tot}} (\hat{N}_{Ri} + \hat{N}_{Li}) \end{bmatrix} \quad (8)$$

$$\hat{\mathbf{G}} = \begin{bmatrix} \hat{X}_G \\ \hat{Y}_G \end{bmatrix} \quad (9)$$

$$\mathbf{d} = \begin{bmatrix} -\sum_{i=1}^{n_{tot}} (\hat{N}_{Ri} + \hat{N}_{Li}) c_i \\ \sum_{i=1}^{n_{tot}} (\hat{N}_{Li} - \hat{N}_{Ri}) \frac{s}{2} \end{bmatrix} \quad (10)$$

Hence, the values of the estimated longitudinal \hat{X}_G and lateral \hat{Y}_G coordinates of the center of gravity G can be computed by simply inverting the C matrix: $\hat{\mathbf{G}} = C^{-1}\mathbf{d}$.

5 Performance of the WIM algorithm

In this chapter the capability of the innovative WIM algorithm in estimating the vertical wheel loads N_{Ri} , N_{Li} and the longitudinal X_G and lateral Y_G coordinates of the vehicle center of gravity G starting from the knowledge of the simulated vertical forces on the sleepers F_{zrk}^{fn} , F_{zlk}^{fn} is shown. The WIM algorithm has been tested with two simulations campaign to verify the accuracy of the procedure when experimental data are not available. In the first simulation campaign, the attention is focused on the influence of vehicle velocity V , vehicle car-body mass M and cut frequency f_n of the physical system. In this chapter the vertical forces on the sleepers $F_{zrk}^{fn}(t) = F_{zrk}^{fn}(x_{rk}, t)$ and $F_{zlk}^{fn}(t) = F_{zlk}^{fn}(x_{lk}, t)$ evaluated through the physical model of the railway track (see chapter 3) are compared with the vertical forces on the sleepers $F_{zrk\ app}^{fn}(t) = F_{zrk\ app}^{fn}(x_{rk}, t)$ and $F_{zlk\ app}^{fn}(t) = F_{zlk\ app}^{fn}(x_{lk}, t)$ estimated by means of the WIM algorithm. The comparison between the calculated and estimated vertical forces is quite important to test the algorithm accuracy when experimental data are not available. Furthermore in this case the measurement errors will be considered (according to chapter 3) to evaluate the algorithm robustness in presence of disturbances. To perform the comparison between simulated F_{zrk}^{fn} , F_{zlk}^{fn} and estimated $F_{zrk\ app}^{fn}$, $F_{zlk\ app}^{fn}$ forces on the sleepers, an extensive simulations campaign has been carried out. In particular the dependence of the relative errors $e_{Ri}^{sim} = \frac{\hat{N}_{Ri}^{sim} - N_{Ri}}{N_{Ri}}$

and $e_{Li}^{sim} = \frac{\hat{N}_{Li}^{sim} - N_{Li}}{N_{Li}}$ on the vehicle speed V , car-body mass M and the cut frequency f_n of the physical system is investigated. In Tab. 1 the variation ranges for the previous quantities are reported together with the resolutions adopted (ΔV , ΔM , Δf_n); the range boundaries take into account both the usual traveling velocity and car-body mass of freight wagons, and the typical frequency range of the studied physical system and measurement chain (where N_v , N_M , N_f represent respectively the number of simulated values of ΔV , ΔM ,

Table 1. Variation ranges of V , M and f_n

Parameter	Min.	Max.	N_{sim}	Δ
Velocity (ms^{-1})	10	40	10	$\Delta V = \frac{(V_{max} - V_{min})}{(N_v - 1)}$
Car-body Mass (t)	20	50	10	$\Delta M = \frac{(M_{max} - M_{min})}{(N_M - 1)}$
Frequency (s^{-1})	10	40	10	$\Delta f_n = \frac{(f_n^{max} - f_n^{min})}{(N_f - 1)}$

Δf_n). In the research activity, the layout of the adopted measurement station consists in $N_m = 3$ measure points on both rail side ($x_{R1} = x_{L1} = 33$ m, $x_{R2} = x_{L2} = 34.2$ m and $x_{R3} = x_{L3} = 38.4$ m). By way of example, Fig. 4 illustrates both simulated $F_{zr2}^{fn}(t)$ and approximated $F_{zr2\ app}^{fn}(t)$ right vertical forces acting on the second measurement point on the right side of the sleeper ($x_{r2} = 34.2$ m) relative to a simulation performed at $V = 40$ ms^{-1} , with a car-body mass $M = 50$ t and with a cut frequency $f_n = 20$ s^{-1} . The figure shows a good agreement between the simulated and estimated quantities, confirming the accuracy of the WIM algorithm. The global performance of the WIM algorithm have been studied by considering the maximum relative error $e_{max}^{sim}(V, M, f_n)$

$$e_{max}^{sim} = \max_{1 \leq i \leq n_{tot}} |max(e_{Ri}^{sim}, e_{Li}^{sim})|. \quad (11)$$

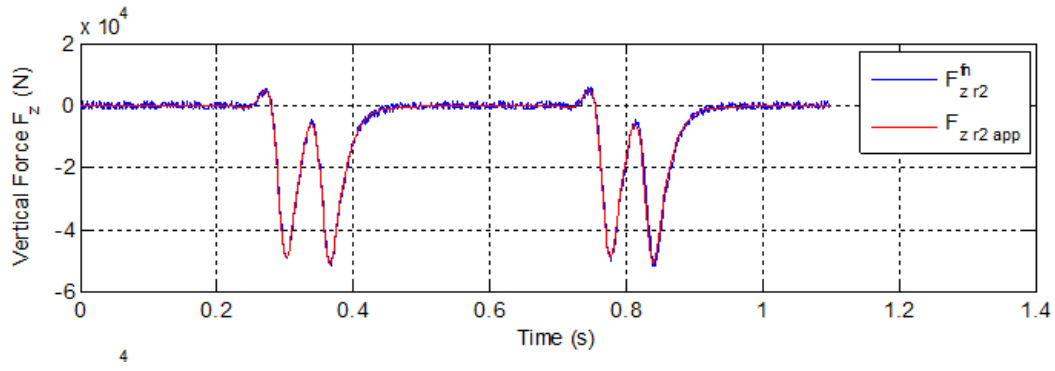


Figure 4. Vertical load acting at $x_{r2} = 34.2$.

The values of the estimated loads \hat{N}_{Ri}^{sim} , \hat{N}_{Li}^{sim} acting on the vehicle wheels evaluated in a test performed with a vehicle speed $V = 40 \text{ m s}^{-1}$ and a car-body mass value $M = 50 \text{ t}$ (the most critical case of all the simulation campaign), are listed for instance in Tab. 2. Tab. 2 also summarizes the relative errors e_{Ri}^{sim} , e_{Li}^{sim} . The algorithm accuracy in estimating the vertical loads (relative errors equal to 0.03 – 1.9%) is mainly due to the capability of correctly describing the global shape of the solutions (both in space and in time). Finally Tab. 2 shows a satisfying accuracy of the WIM algorithm even for relatively low values of f_n .

Table 2. Estimated loads, $\hat{N}_{Ri}^{sim}, \hat{N}_{Li}^{sim}$: $V = 40 \text{ m/s}$, $M = 50 \text{ t}$.

Cut frequency f_n Hz	Parameter	Value kN	Parameter	Value %
10	\hat{N}_{R1}^{sim}	75.4	e_{R1}^{sim}	1.4%
40		76.8		0.2%
10	\hat{N}_{L1}^{sim}	75.4	e_{L1}^{sim}	1.7%
40		76.7		0.03%
10	\hat{N}_{R2}^{sim}	75.9	e_{R2}^{sim}	0.7%
40		76.7		0.2%
10	\hat{N}_{L2}^{sim}	76.2	e_{L2}^{sim}	0.4%
40		76.1		0.5%
10	\hat{N}_{R3}^{sim}	75.2	e_{R3}^{sim}	1.7%
40		76.4		0.2%
10	\hat{N}_{L3}^{sim}	75.1	e_{L3}^{sim}	1.9%
40		76.5		0.4%
10	\hat{N}_{R4}^{sim}	75.3	e_{R4}^{sim}	1.7%
40		76.8		0.1%
10	\hat{N}_{L4}^{sim}	75.7	e_{L4}^{sim}	1.3%
40		76.7		0.06%

To test the accuracy in the estimation of the longitudinal X_G and lateral Y_G coordinates of the vehicle center of gravity G , a second simulation campaign has been performed. The actual longitudinal X_G and lateral Y_G positions have been varied according to Tab. 3 (with resolutions equal to N_x and N_y). The campaign has been performed with the following dynamical parameters: $M = 50 \text{ t}$, $f_n = 20 \text{ s}^{-1}$ and $V = 40 \text{ m s}^{-1}$. The accuracy in the estimation of the vertical loads, makes the WIM algorithm quite suitable also for the estimation of the longitudinal X_G and lateral Y_G position of the center of mass of the vehicle. Some results, in terms of absolute errors in estimating X_G and Y_G , are reported for example in Tab. 4.

Table 3. Variation ranges of X_G and Y_G

Parameter	Min.	Max.	N_{sim}	Δ
X_G (m)	-3.0	3.0	10	$\Delta X_G = \frac{(X_{Gmax} - X_{Gmin})}{(N_x - 1)}$
Y_G (m)	-0.5	0.5	10	$\Delta Y_G = \frac{(Y_{Gmax} - Y_{Gmin})}{(N_y - 1)}$

Table 4. Estimation of X_G and Y_G - $M = 50t$, $f_n = 20 \text{ s}^{-1}$ and $V = 40 \text{ ms}^{-1}$

Simulation	e_{X_G}	e_{Y_G}
$X_G = 0.0\text{m}$ $Y_G = 0.0\text{m}$	0.009 mm	0.003 mm
$X_G = 3.0\text{m}$ $Y_G = 0.5\text{m}$	0.021 mm	0.010 mm
$X_G = -3.0\text{m}$ $Y_G = 0.5\text{m}$	0.020 mm	0.011 mm
$X_G = 3.0\text{m}$ $Y_G = -0.5\text{m}$	0.018 mm	0.010 mm
$X_G = -3.0\text{m}$ $Y_G = -0.5\text{m}$	0.022 mm	0.014 mm

6 Conclusions and further developments

In this paper the authors presented an innovative WIM algorithm with the aim of estimating the vertical wheel loads \hat{N}_{Ri} , \hat{N}_{Li} and the longitudinal \hat{X}_G and lateral \hat{Y}_G coordinates of the gravity center of railway vehicles. The WIM algorithm developed by the authors can work both with real experimental and simulated data (when experimental data are not available). The algorithm is based on the measurement of the vertical forces on the sleepers F_z performed through force sensitive elements placed over the sleepers in the section corresponding to the rail baseplate/pads. These physical quantities are processed by means of suitable estimation procedures derived from the least squares minimization that allow the calculation of the loads \hat{N}_{Ri} , \hat{N}_{Li} and of the position \hat{X}_G , \hat{Y}_G of the center of mass G of the vehicle. The results of the new WIM algorithm highlighted a good agreement between the estimated quantities and the simulated data, confirming the good accuracy of the procedure. Concerning the future developments, the improvements will regard the adoption of other estimation procedures (like weighted least square optimization (WLSO) and nonlinear least square optimization (NLSO) and other possible physical inputs of the algorithm besides the vertical forces on the sleepers F_z (like generic stresses σ and deformations ε directly measured on the rails). The goal of the improved algorithms will be also the estimation of other geometrical and physical characteristics of the railway vehicle. From an experimental point of view, experimental tests are currently being carried out by Ansaldo STS and ECM Spa to further validate the WIM algorithm. Moreover a real prototype of the measure station is being now designed and will be soon assembled on a suitable railway track. The prototype will aim at testing the accuracy and the robustness of the WIM algorithm together with the effectiveness of the various measure station layouts.

REFERENCES

- [1] S. Falomi, M Malvezzi, and E. Meli. Multibody modeling of railway vehicles: innovative algorithms for the detection of wheel-rail contact points. *Wear*, 271(1-2):453–461, 2011.
- [2] M. Ignesti, A. Innocenti, L. Marini, E. Meli, L. Pugi, and A. Rindi. Development of an innovative weigh in motion system for railways vehicles. In *Proceedings of the Multibody Dynamics Congress (ECCOMAS)*, Zagreb, Croatia, 2013.
- [3] S. Iwnicki. *Handbook of Railway Vehicle Dynamics*. Taylor and Francis, 2006.
- [4] S. Iwnicki. *The Manchester Benchmarks for Rail Vehicle Simulators*. Swets and Zeitlinger, Lisse, Netherland, 1999, 2008.
- [5] J. J. Kalker. *Three-dimensional Elastic Bodies in Rolling Contact*. Kluwer Academic Publishers, Dordrecht, Netherlands, 1990.
- [6] C. Kelley. *Iterative methods for linear and nonlinear equations*. SIAM, Philadelphia, PA, USA, 1995.

- [7] J. Kisilowski and K. Knothe. *Advanced railway vehicle-system dynamics*. Wydawnictwa Naukowo-Techniczne, Warsaw, Poland, 1991.
- [8] E. Meli, S. Falomi, M. Malvezzi, and A. Rindi. Determination of wheel - rail contact points with semianalytic methods. *Multibody System Dynamics*, 20(4):327–358, 2008.
- [9] E. Meli and L. Pugi. Preliminary development, simulation and validation of a weigh in motion system for railway vehicles. *Meccanica*, 48(10):2541–2565, 2013.
- [10] J. Nocedal and S. Wright. *Numerical optimization*. Springer Series in Operation Research, Springer, Berlin, Germany, 1999.
- [11] K. Sekula and P. Kolakowski. Identification of dynamic loads generated by trains in motion using piezoelectric sensors. In *Proceedings of ISMA*, Leuven, Belgium, 2010.
- [12] L. F. Shampine and M. W. Reichelt. The matlab ode suite. *SIAM Journal of Scientific Computation*, 18:1–22, 1997.